

---

# Optimal Solution Predictions for Mixed Integer Programs

---

**Jian-Ya Ding**

Artificial Intelligence Department,  
Zhejiang Cainiao Supply Chain  
Management Co., Ltd  
jianya.djy@cainiao.com

**Chao Zhang**

Artificial Intelligence Department,  
Zhejiang Cainiao Supply Chain  
Management Co., Ltd  
chao.zc@cainiao.com

**Lei Shen**

Artificial Intelligence Department,  
Zhejiang Cainiao Supply Chain  
Management Co., Ltd  
kenny.sl@cainiao.com

**Shengyin Li**

Artificial Intelligence Department,  
Zhejiang Cainiao Supply Chain  
Management Co., Ltd  
shengyin.lsy@cainiao.com

**Bing Wang**

Artificial Intelligence Department,  
Zhejiang Cainiao Supply Chain  
Management Co., Ltd  
lingfeng.wb@cainiao.com

**Yinghui Xu**

Artificial Intelligence Department,  
Zhejiang Cainiao Supply Chain  
Management Co., Ltd  
renji.xyh@taobao.com

**Le Song**

Computational Science and Engineering  
College of Computing  
Georgia Institute of Technology  
lsong@cc.gatech.edu

## Abstract

Mixed Integer Programming (MIP) is one of the most widely used modeling techniques to deal with combinatorial optimization problems. In many applications, a similar MIP model is solved on a regular basis, maintaining remarkable similarities in model structures and solution appearances but differing in formulation coefficients. This offers the opportunity for machine learning method to explore the correlations between model structures and the resulting solution values. To address this issue, we propose to represent an MIP instance using a tripartite graph, based on which a Graph Convolutional Network (GCN) is constructed to predict solution values for binary variables. The predicted solutions are used to generate a local branching cut to the model which accelerate the solution process for MIP. Computational evaluations on 8 distinct types of MIP problems show that the proposed framework improves the performance of a state-of-the-art open source MIP solver significantly in terms of running time and solution quality.

## 1 Introduction

*Mixed Integer Programming* (MIP) is widely used to solve vast *combinatorial optimizations* (CO) in the field of *Operations Research* (OR). The existence of integer variables endows MIP formulations

with the ability to capture the discrete nature of many real world decisions. Applications of MIP includes production scheduling, vehicle routing, facility location, airline crew scheduling, to mention only a few. In many real-world settings, homogeneous MIP instances with similar scales and combinatorial structures are optimized repeatedly, but being treated as completely new tasks. These MIP models across days share remarkable similarities in model structures and solution appearances, which motivates us to integrate *Machine Learning* (ML) method to explore correlations between an MIP model's structure and its solution values to improve the solver's performance.

Identifying correlations between problem structures and solution values is not new, and is widely used as guidelines for heuristics design for CO problems. These heuristic methods are usually human-designed priority rules to guide the search directions to more promising regions in solution space. For example, the nearest neighbor algorithm for traveling salesman problem (TSP) constructs a heuristic solution by choosing the nearest unvisited node as the salesman's next move, based on the observation that two distantly distributed nodes are unlikely to appear consecutively in the optimal route. Similar examples include the shortest processing time first heuristic for flow shop scheduling, the saving heuristic for vehicle routing, the first fit algorithm for bin packing, among many others. A major drawback of heuristics design using problem-specific knowledge is the lack of generalities to other problems, where new domain knowledge has to be re-identified.

MIP models can describe CO problems of various types using a standard formulation strategy  $z = \min_{A\mathbf{x} \leq \mathbf{b}, \mathbf{x} \in \mathcal{X}} \mathbf{c}^T \mathbf{x}$ , differing only in model coefficients  $\mathbf{A}$ ,  $\mathbf{b}$  and  $\mathbf{c}$ . This makes it possible to explore connections between problem structures and the resulting solution values without prior domain knowledge. Predicting solution values of general integer variables in MIP is a difficult task. Notice that most MIP models are binary variables intensive<sup>1</sup>, a natural way to explore hidden information in the model is to treat solution value prediction of binary variables as binary classification tasks. Major challenges in solution prediction lies in the implicit correlations among decision variables, since a feasible solution  $\mathbf{x}$  is restricted by constraints in MIP, i.e.,  $A\mathbf{x} \leq \mathbf{b}$ . Rather than predicting each decision variable value isolatedly, we propose a tripartite graph representation of MIP and use graph embedding to capture connections among the variables. Note that none of the two variable nodes are directly linked in the trigraph, but can be neighbors of distance 2 if they appear in the same constraint in the MIP formulation. Correlations among variables are reflected in embeddings of the trigraph where each vertex maintains aggregate feature information from its neighbors.

Incorporating solution prediction results in MIP solving process is not trivial. In fact, false prediction of a single decision variable can sometimes lead to infeasibility of the entire problem. Instead of utilizing the predicted solutions directly, we identify decision variables that are predictable and stable and use this information to guide the Branch and Bound (B&B) tree search to emphasize on unpredictable variables to accelerate solving convergence. This is achieved by a novel labelling mechanism on the training instances, where a sequence of feasible solutions are generated by an iterated proximity search method. *Stable* decision variables, of which the value remain unchanged across these solutions, are recorded. It is noticeable that although obtaining optimal solutions can be a difficult task, the stable variables can be viewed as an easy-to-predict part that reflects the MIP's local optimality structure. This labelling mechanism is inspiring especially for difficult MIP instances when solving them to optimality is almost impossible.

The overall framework of solution prediction based MIP solving can be summarized as follows:

**Training data generation:** For a certain type of CO problem, generate a set of  $p$  MIP instances  $\mathcal{I} = \{I_1, \dots, I_p\}$  of similar scale from the same distribution  $\mathbb{D}$ . For each  $I_i \in \mathcal{I}$ , collect the corresponding variable features, constraint features and edge features, and use the iterated proximity search method to generate solution labels for each binary variable in  $I_i$ .

**GCN model training:** For each  $I_i \in \mathcal{I}$ , generate a trigraph from its MIP formulation and train a Graph Convolutional Network (GCN) for solution value prediction of each binary variable.

**Application of solution prediction:** For a new MIP instance  $I$  from  $\mathbb{D}$ , collect features, build the trigraph and use the GCN model to make solution value predictions, based on which an initial local branching cut heuristic is applied to solve  $I$ .

---

<sup>1</sup>Take the benchmark set of MIPLIB 2017 [15] as an example, among all 240 MIP benchmark instances, 164 of them are Binary Integer Linear Programming (BILP) problems, and 44 out of the 76 remaining are imbalanced in the sense that binary variables account for more than 90% of all integer variables.

## 2 Related work

With a similar motivation, there are some recent attempts that consider integration of ML and OR for solving CO problems. Dai et al. [5] combined reinforcement learning and graph embedding to learn greedy construction heuristics for several optimization problems over graphs. Li et al. [13] trained a graph convolutional network to estimate the likelihood that a vertex in a graph appears in the optimal solution. Selsam et al. [18] proposed a message passing neural network named NeuroSAT to solve SAT problems via a supervised learning framework. Vinyals et al. [20], Kool et al. [10, 11] and Nazari et al. [16] trained Pointer Networks (or its variants) with recurrent neural network (RNN) decoder to solve permutation related optimization problems over graphs, such as Traveling Salesman Problem (TSP) and Vehicle Routing Problem (VRP). Quite different from their settings, our solution prediction framework does not restrict to certain graph based problems, but can adapt to a variety of CO problems using a standard MIP formulation.

Quite related to our work, there is an increasing concern on using ML techniques to enhance MIP solving performance. Alvarez et al. [2], Marcos et al. [14], and Khalil et al. [9] tried to use learning-based approach to imitate the behavior of the so-called strong branching method, a node-efficient but time-consuming branching variable selection method in the B&B search tree. He et al. [7] used imitation learning to train a node selection and a node pruning policy to speed up tree search in the B&B process. Khalil et al. [8] used binary classification to predict whether a primal heuristic will succeed at a given node and then decide whether to run a heuristic at that node. Kruber et al. [12] proposed a supervised learning method to decide whether a Danzig-Wolfe reformulation should be applied and which decomposition to choose among all possibles. Interested readers can refer to Bengio et al. [3] for a comprehensive survey on the use of machine learning methods in CO.

The proposed MIP solving framework is different from previous work in two aspects:

**Generalization:** Previous solution generation method for CO usually focus on problems with certain solution structures. For example, applications of Pointer Networks [20, 11] are only suited for sequence-based solution encoding, and reinforcement learning [5, 13] type decision making is based on the assumption that a feasible solution can be obtained by sequential decisions. In contrast, the proposed framework do not limit to problems of certain types, but is applicable to all CO problems that can be modeled as MIPs. This greatly enlarges the applicable area of the proposed framework.

**Representation:** Previous applications of ML techniques to enhance MIP solving performance mainly use hand-crafted features and make predictions on each variable independently. Notice that the solution value of an variable is strongly correlated to the objective function and the constraints it participates in, we build a novel tripartite graph representation for MIP, based on which graph embedding technique is applied to extract correlations among variables, constraints and the objective function without human intervene.

## 3 The Solution Framework

Consider an MIP problem instance  $I_0$  of the following general form:

$$\min \quad \mathbf{c}^T \mathbf{x} \quad (1)$$

$$\text{s.t.} \quad \mathbf{A}\mathbf{x} \leq \mathbf{b}, \quad (2)$$

$$x_j \in \{0, 1\}, \forall j \in \mathcal{B}, \quad (3)$$

$$x_j \in \mathbb{Z}, \forall j \in \mathcal{Q}, \quad x_j \geq 0, \forall j \in \mathcal{P}, \quad (4)$$

where the index set of decision variables  $\mathcal{U} := \{1, \dots, n\}$  is partitioned into  $(\mathcal{B}, \mathcal{Q}, \mathcal{P})$ , and  $\mathcal{B}, \mathcal{I}, \mathcal{P}$  are the index set of binary variables, general integer variables and continuous variables, respectively. The main task here is to predict the probability that a binary variable  $x_j, j \in \mathcal{B}$  to take value 1 (or zero) in the optimal solution. Next we describe in detail the tripartite graph representation of MIP, the GCN model structure, and how solution prediction results are incorporated to accelerate MIP solving.

### 3.1 Graph Representation for MIP

Our main idea is to use a tripartite graph  $\mathcal{G} = \{\mathcal{V}, \mathcal{E}\}$  to represent an input MIP instance  $I_0$ . In particular, objective function coefficients  $\mathbf{c}$ , constraints right-hand-side (RHS) coefficients  $\mathbf{b}$  and

coefficients matrix  $\mathbf{A}$  information is extracted from  $I_0$  to build the graph. Vertices and edges in the graph are detailed as follows and graphically illustrated in Fig 1.

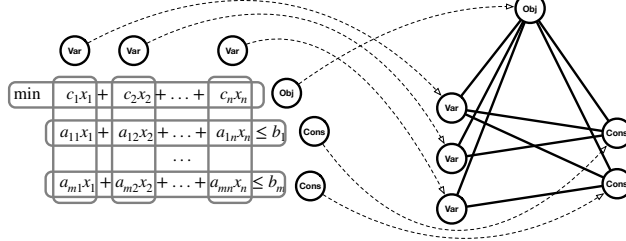


Figure 1: Transformation of an MIP instance to a tripartite graph

**Vertices:**

- 1) the set of decision variable vertices  $\mathcal{V}_V$ , each of which corresponds to a binary variable in  $I_0$ .
- 2) the set of constraint vertices  $\mathcal{V}_C$ , each of which corresponds to a constraint in  $I_0$ .
- 3) an objective function vertex  $o$ .

**Edges:**

- 1)  $v-c$  edge: there exists an edge between  $v \in \mathcal{V}_V$  and  $c \in \mathcal{V}_C$  if the corresponding variable of  $v$  has a non-zero coefficient in the corresponding constraint of  $c$  in the MIP formulation.
- 2)  $v-o$  edge: for each  $v \in \mathcal{V}_V$ , there exists an edge between  $v$  and  $o$ .
- 3)  $c-o$  edge: there exists an edge between  $c \in \mathcal{V}_C$  and  $o$  if  $c$  is active in the MIP's root LP relaxation.

**Remark.** The presented trigraph representation not only captures connections among the variables, constraints and objective functions, but maintains the detailed coefficients numerics in its structure as well. In particular, non-zero entries in coefficient matrix  $\mathbf{A}$  are included as features of  $v-c$  edges, entries in objective coefficients  $c$  as features of  $v-o$  edges, and entries in RHS coefficients  $b$  as features of  $c-o$  edges. Note that the constraint RHS coefficients  $b$  are correlated to the objective function by viewing LP relaxation of  $I_0$  from a dual perspective.

### 3.2 Solution Prediction for MIP

We describe in Algorithm 1 the overall forward propagation prediction procedure based on the trigraph. The model has three stages: 1) a projection layer of same embedding size for each node so that node feature has the same dimension (line 1-3 in the algorithm). 2) a graph attention network to transform node information among connected nodes (line 4-10). 3) two fully-connected layers between variable nodes and the output layer after several information transitions (line 11).

---

**Algorithm 1** Graph Convolutional Network (forward propagation)

---

**Input:** Graph  $\mathcal{G} = \{\mathcal{V}, \mathcal{E}\}$ ; Input features  $\{\mathbf{x}_j, \forall j \in \mathcal{V}\}$ ; Number of transition iterations  $T$ ; Weight matrices  $\mathbf{W}^t, \forall t \in \{1, \dots, T\}$  for graph embedding; Output layer weight matrix  $\mathbf{W}^{\text{out}}$ ; Non-linearity  $\sigma$ ; Neighborhood function  $\mathcal{N}$ ; Attention coefficients  $\alpha$ .

**Output:** Predicted value of all variable:  $z_v, \forall v \in \mathcal{V}_V$ .

- 1:  $\mathbf{h}_v^0 \leftarrow \text{EMBEDDING}(\mathbf{x}_v), \forall v \in \mathcal{V}_V$
- 2:  $\mathbf{h}_c^0 \leftarrow \text{EMBEDDING}(\mathbf{x}_c), \forall c \in \mathcal{V}_C$
- 3:  $\mathbf{h}_o^0 \leftarrow \text{EMBEDDING}(\mathbf{x}_o)$
- 4: **for**  $t = 1, \dots, T$  **do**
- 5:    $\mathbf{h}_o^t \leftarrow \sigma \left( \mathbf{W}_{V_o}^t \cdot \text{CONCAT} \left( \mathbf{h}_o^{t-1}, \sum_{v \in \mathcal{V}_V \cap \mathcal{N}(o)} \alpha_{vo} \mathbf{h}_v^{t-1} \right) \right)$
- 6:   **for**  $c$  in  $\mathcal{C}$  **do** :
- 7:      $\mathbf{h}_c^t \leftarrow \sigma \left( \mathbf{W}_{V_c}^t \cdot \text{CONCAT} \left( \sigma \left( \mathbf{W}_{oC}^t \cdot \text{CONCAT} \left( \mathbf{h}_o^t, \mathbf{h}_c^{t-1} \right) \right), \sum_{v \in \mathcal{V}_V \cap \mathcal{N}(c)} \alpha_{vc} \mathbf{h}_v^{t-1} \right) \right)$
- 8:      $\mathbf{h}_o^t \leftarrow \sigma \left( \mathbf{W}_{C_o}^t \cdot \text{CONCAT} \left( \mathbf{h}_o^t, \sum_{c \in \mathcal{V}_C \cap \mathcal{N}(o)} \alpha_{co} \mathbf{h}_c^{t-1} \right) \right)$
- 9:   **for**  $v$  in  $\mathcal{V}$  **do** :
- 10:      $\mathbf{h}_v^t \leftarrow \sigma \left( \mathbf{W}_{Cv}^t \cdot \text{CONCAT} \left( \sigma \left( \mathbf{W}_{oV}^t \cdot \text{CONCAT} \left( \mathbf{h}_o^t, \mathbf{h}_v^{t-1} \right) \right), \sum_{c \in \mathcal{V}_C \cap \mathcal{N}(v)} \alpha_{cv} \mathbf{h}_c^t \right) \right)$
- 11:      $z_v \leftarrow \sigma \left( \mathbf{W}^{\text{out}} \cdot \text{CONCAT} \left( \mathbf{h}_v^0, \mathbf{h}_v^T \right) \right), \forall v \in \mathcal{V}_V$

---

Nodes' representations in the tripartite graph are updated via a 4-step procedure. In the first step (line 5 in Algorithm 1), the objective node  $o$  aggregates the representations of all variable nodes

$\{\mathbf{h}_v, v \in \mathcal{V}_V\}$  to update its representation  $\mathbf{h}_o$ . In the second step (line 7),  $\{\mathbf{h}_v, v \in \mathcal{V}_V\}$  and  $\mathbf{h}_o$  are used to update representation of their neighboring constraint node  $c \in \mathcal{V}_C$ . In the third step (line 8), representations of constraints  $\{\mathbf{h}_c, c \in \mathcal{V}_C\}$  are aggregated to update  $\mathbf{h}_o$ , while in the fourth step (line 10)  $\{\mathbf{h}_c, c \in \mathcal{V}_C\}$  and  $\mathbf{h}_o$  are combined to update  $\{\mathbf{h}_v, v \in \mathcal{V}_V\}$ . See Fig. 2 for an illustration of information transition flow in the trigraph.

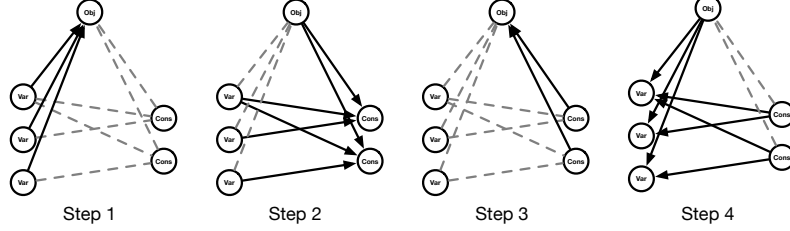


Figure 2: Information transition flow in the trigraph convolutional layer

The information transitions run consecutively as follows: Step 1, transform variable nodes information to the objective node; Step 2, transform the objective and variable nodes information to constraint nodes; Step 3, transform constraint nodes information to the objective node; Step 4, transform the objective node and constraint nodes information to variable nodes;

The intuition behind Algorithm 1 is that at each iteration, a variable node can incrementally gather more aggregation information from its neighboring nodes, which correspond to the related constraints and variables in the MIP formulation. It is worth mentioning that the above transitions only extract connection relations among the nodes, ignoring the detailed coefficients numerics  $\mathbf{A}$ ,  $\mathbf{b}$  and  $\mathbf{c}$  in MIP. To enhance the representation ability of our model, we include an attention mechanism to import information from the coefficients values.

**Attention Mechanism:** A distinct feature in the tripartite graph structure is the heterogeneities in nodes and arcs. Rather than using a shared linear transformation (i.e., weight matrix) for all nodes [19], we consider different transformations in each step of graph embedding updates, reflecting the importance of feature of one type of node on the other. In particular, given node  $i$  of type  $T_i$  and node  $j$  of type  $T_j$ , the attention coefficient which indicates the importance of node  $i \in \mathcal{V}$  from its neighbor  $j \in \mathcal{N}(i)$  is computed as:

$$\alpha_{ij} = \sigma \left( \mathbf{W}_{T_i, T_j}^{\text{att}} \cdot \text{CONCAT} (\mathbf{h}_i, \mathbf{h}_{e_{ij}}, \mathbf{h}_j) \right), \quad (5)$$

where  $\mathbf{h}_i, \mathbf{h}_j, \mathbf{h}_{e_{ij}}$  are embeddings of node  $i, j \in \mathcal{V}$  and edge  $(i, j) \in \mathcal{E}$  respectively, and  $\mathbf{W}_{T_i, T_j}^{\text{att}}$  is the attention weight matrix between type  $T_i$  and  $T_j$  nodes. For each  $i \in \mathcal{V}$ , the attention coefficient is normalized cross over all neighbor nodes  $j \in \mathcal{N}(i)$  using a softmax function. With this attention mechanism, MIP coefficients information in  $\mathbf{A}$ ,  $\mathbf{b}$  and  $\mathbf{c}$  (all of which contained in the feature vector of the edges) are incorporated to reflect edge connection importance in the graph.

### 3.3 Prediction-Based MIP Solving

Next, we introduce how the solution value prediction results are utilized to improve MIP solving performance. One approach is to add a local branching type initial cut to the MIP model to reduce the search space of feasible solutions. This method aim to identify decision variables that are predictable and stable, and guide the B&B tree search to emphasize on unpredictable variables which accelerate solving convergence while maintaining near optimality.

Let  $\hat{x}_j$  denotes the predicted solution value of binary variable  $x_j, j \in \mathcal{B}$ , and let  $\mathcal{S} \subset \mathcal{B}$  denotes an subset of indices of binary variables. A local branching initial cut to the model is defined as:

$$\sum_{j \in \mathcal{S}: \hat{x}_j^k = 0} x_j + \sum_{j \in \mathcal{S}: \hat{x}_j^k = 1} (1 - x_j) \leq \phi, \quad (6)$$

where  $\phi$  is a problem parameter that controls the maximum distance from a new solution  $\mathbf{x}$  to the predicted solution  $\hat{\mathbf{x}}$ . Adding cuts with respect to subset  $\mathcal{S}$  rather than  $\mathcal{B}$  is due to the unpredictable nature of unstable variables in MIP solutions. Therefore, only those variables with high probability to take value 0 or 1 are included in  $\mathcal{S}$ . It is worth mentioning that for the extreme case of  $\phi$  equals 0, the initial cut is equivalent to fixing variables with indices in  $\mathcal{S}$  at their predicted values.

## 4 Data Collection

**Features:** An ideal feature collection procedure should capture sufficient information to describe the solution process, and being of low computational complexity as well. A good trade off between these two concerns is to collect features at the root node of the B&B tree, where the problem has been presolved to eliminate redundant variables and constraints and the LP relaxation is solved. In particular, we collect for each instance 3 types of problem features, i.e., variable features, constraint features and edge features. Features descriptions are summarized in Table 1 in Appendix A.

As presented in the feature table, features of variables and constraints can be divided into three categories: basic features, LP features and structure features. The structure features (most of which can be found in [2, 9]) are usually hand-crafted statistics to reflect correlations between variables and constraints. It is noticeable that our tripartite graph neural network model can naturally capture these correlations without human expertise and can generate more advanced structure information to improve prediction accuracy. This will be verified in the computational evaluations section.

**Labels:** To make predictions on solution values of binary variables, an intuitive labeling scheme for the variables is to label them with the optimal solution values. Note, however, obtaining optimal solutions for medium or large scale MIP instances can be very time-consuming or even an impossible task. This implies that labeling with optimal solutions can only be applied to solvable MIP instances, which limit the applications of the proposed framework.

Instead of collecting optimal solutions, we propose to identify *stable* and *unstable* variables in solutions. This is motivated by the observation that solution values of the majority of binary decision variables remain unchanged across a series of different feasible solutions. To be specific, given a set of  $K$  solutions  $\{\bar{x}^1, \dots, \bar{x}^K\}$  to an MIP instance  $I_0$ , a binary variable  $x_j$  is defined as unstable if there exists some  $k_1, k_2 \in \{1, \dots, K\}$  such that  $x_j^{k_1} \neq x_j^{k_2}$ , and as stable otherwise. Although obtaining optimal solutions might be a difficult task, the stable variables can be viewed as an easy-to-predict part in the (near) optimal solutions. To generate a sequence of solutions to an instance, we use the so-called proximity search method [6]. Starting from some initial solution  $\bar{x}^k$  with objective value  $\mathbf{c}^T \bar{x}^k$ , a neighborhood solution with the objective value improvement being at least  $\delta$  can be generated by solving the following optimization:

$$\min \sum_{j \in \mathcal{B}: \bar{x}_j^k = 0} x_j + \sum_{j \in \mathcal{B}: \bar{x}_j^k = 1} (1 - x_j) \quad (7)$$

$$\text{s.t. } \mathbf{c}^T \mathbf{x} \leq \mathbf{c}^T \bar{x}^k - \delta, \quad (8)$$

$$\mathbf{A} \mathbf{x} \leq \mathbf{b}, \quad (9)$$

$$x_j \in \{0, 1\}, \forall j \in \mathcal{B}, \quad x_j \in \mathbb{Z}, \forall j \in \mathcal{G}, \quad x_j \geq 0, \forall j \in \mathcal{C}. \quad (10)$$

where the objective function represents the distance between  $\bar{x}^k$  and a new solution  $\mathbf{x}$ . Note that the above optimization is computationally tractable since solving process can terminate as soon as a feasible solution is found. By iteratively applying this method, we obtain a series of improving feasible solutions to the original problem. Stable binary variables are labeled with their solution values while the unstable variables are marked as unstable and discarded from the training set.

**Remark.** The logic behind the stable variable labelling scheme is to explore local optimality patterns rather than global optimality. In each iteration of proximity search, a neighboring better solution is found, with a few flips on solution values of the binary variables. Performing such a local search step for many rounds can identify local minimum patterns which reflects domain knowledge of the CO problem. Take the Traveling Salesman Problem (TSP) as an example. Let a binary variable  $z_{jl}$  defines whether node  $l$  is visited immediately after node  $j$ . If node  $j$  and  $l$  are geometrically faraway from each other,  $z_{jl}$  is likely to be zero in all the solutions generated by proximity search, and being recorded by our labelling scheme, which reflects the underlying local optimality knowledge for TSP.

## 5 Experimental Evaluations

**Setup.** To evaluate the proposed framework, we modify the state-of-the-art open source MIP solver SCIP 6.0.0 [1] for data collection and solution quality comparison. The GCN model is built using the Tensorflow API. All experiments were conducted on a cluster of three 4-core machines with Intel 2.2 GHz processors and 16 GB RAM.

**Instances.** To test the effectiveness and generality of our solution prediction method in this scenario, we generate problem instances of 8 distinct types: *Fixed Charge Network Flow* (FCNF), *Capacitated Facility Location* (CFL), *Generalized Assignment* (GA), *Maximal Independent Set* (MIS), *Multi-dimensional Knapsack* (MK), *Set Covering* (SC), *Traveling Salesman Problem* (TSP) and *Vehicle Routing Problem* (VRP). These problems are the most commonly visited NP-hard combinatorial optimizations in OR and are quite general because they differ significantly in MIP structures and optimal solution structures. For each problem type, 200 MIP instances of similar scales are generated. Detailed MIP formulation and instance parameters of each type are included in Appendix B.

**Data collection.** In terms of feature collection, we implemented a feature extraction plugin embedded in the branching procedure of SCIP. In particular, variable features, constraint features and edge features are collected right before the first branching decision is made at the root node, where presolving process and the root LP relaxation has completed. No further exploration of the B&B search tree is needed for data collection and thus the feature collection process terminates at the root node. Construction of the tripartite graph is also completed at the root node where SCIP is working with a transformed MIP model such that redundant variables and constraints have been removed. In terms of label collection, we applied the proximity search method to label stable binary variables. Each proximity search iteration terminates as soon as a feasible solution is found.

## 5.1 Results of Solution Prediction

We demonstrate the effectiveness of the proposed GCN model on solution prediction accuracy against two classical classifiers: Logistics Regression (LR) [17] and XGBoost (XGB)<sup>2</sup> [4]. Noting that solution values of binary variables are usually highly imbalanced (due to the one-hot encoding convention in MIP formulation for CO problems), we use the Average Precision (AP) metric [21] to justify the results of different classifiers.

Table 1: Comparisons on the average precision metric

Instances	Basic features			Basic&structure features			All features		
	LR	XGB	GCN	LR	XGB	GCN	LR	XGB	GCN
FCNF	0.0888	0.0993	<b>0.2614</b>	0.2291	0.2749	<b>0.3169</b>	0.7852	0.7867	<b>0.7880</b>
CFL	0.2939	0.4485	<b>0.5899</b>	0.2884	0.5669	<b>0.6286</b>	0.8458	0.8460	<b>0.8500</b>
GA	0.4046	0.4991	<b>0.7440</b>	0.6325	0.7495	<b>0.7969</b>	0.9188	0.9362	<b>0.9373</b>
MIS	0.2967	0.2816	<b>0.3545</b>	0.2988	0.2885	<b>0.3366</b>	0.3220	0.2966	<b>0.3254</b>
MK	0.5614	0.5242	<b>0.8402</b>	0.8034	0.8077	<b>0.8427</b>	<b>0.9317</b>	0.9240	0.9270
SC	0.7441	0.7470	<b>0.7482</b>	0.7326	0.7480	<b>0.7532</b>	0.9357	0.9588	<b>0.9590</b>
TSP	0.3295	0.3265	<b>0.3584</b>	0.3464	0.3488	<b>0.3526</b>	<b>0.4139</b>	0.4009	0.4132
VRP	0.3825	0.3907	<b>0.4027</b>	0.4003	0.4203	<b>0.4241</b>	0.4495	0.4373	<b>0.4587</b>
Average	0.3877	0.4146	<b>0.5374</b>	0.4664	0.5256	<b>0.5564</b>	0.7003	0.6983	<b>0.7073</b>

Table 1 describes the AP value comparison results for the three classifiers under three settings: using only basic features, using basic&structure features, and using all features respectively. It is observed that the proposed GCN model outperforms two baseline classifiers in all settings. The performance advantage is particularly significant in the basic feature columns (0.5374 by GCN against 0.3877 by LR and 0.4146 by XGB), where only raw coefficient numerics in MIP are used for prediction. Another notable statistics in the table are that the GCN model with only basic features is in average superior to LR and XGB models with basic&structure features, indicating that the proposed embedding framework can extract more information compared to hand-crafted structure features used in the literature [2, 9]. For comparisons in the all features column, the advantage of GCN is less significant due to the reason that high level MIP structure information is also captured in its LP features.

To help illustrate the predictability in solution values for problems of different types, we present in Fig.3 the detailed accuracy curve for each of the 8 problem types using GCN model with all features. Fig.3(a) is the standard precision-recall curve from which the statistics in Table 1 are calculated. Fig.3(b) depicts the prediction accuracy if we only predict a certain percentage of most predictable binary variables, of which the output probability by GCN is most extreme. It can be observed from

<sup>2</sup>For LR and XGB, only variable features are used for prediction since they do not maintain MIP formulation structure in their model.

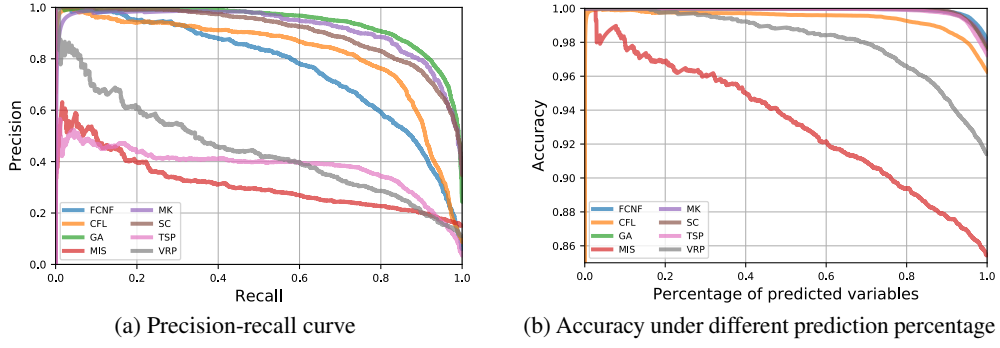


Figure 3: Prediction accuracy results for the 8 types of MIP problems

the figure that solution values of most considered MIP problems are fairly predictable, with a 100% accuracy if we make solution value prediction on the top 50-80% most predictable variables. Among the tested problem types, solution values to MIS problem instances are most unpredictable, which is consistent with intuition that the set of nodes with maximal cardinality in a graph may be multiple and can be hardly obtained with local optimality information in our labelling scheme.

## 5.2 Comparisons of solution quality

To evaluate the value of incorporating solution predictions in MIP solving, we compare the performance of prediction-based MIP solving against that of the solver’s default setting. For each problem type, 10 testing MIP instances (of similar scales and with the same coefficients distribution) are generated. Since optimal solutions or tight lower bounds are difficult to obtain within a reasonable time limit, we use the primal gap metric and the primal integral metric [8] to capture solver’s performance. The primal gap metric reports the relative gap in objective values of the current solution  $x$  to the best known solution  $x^*$ , and primal integral records the average primal gap in the solution process.

Table 2: Comparisons of solution quality

	Primal Gap (%)					Primal Integral				
	DEF1*	DEF2	DEF5	DEF10	GCN	DEF1	DEF2	DEF5	DEF10	GCN
FCNF	4.585	3.991	0.782	0.327	<b>0.000</b>	444.6	360.6	203.0	186.9	<b>9.8</b>
CFL	1.856	1.271	0.280	<b>0.050</b>	0.233	163.7	123.0	101.0	84.9	<b>37.1</b>
GA	5.207	4.972	4.755	3.901	<b>0.000</b>	689.3	548.8	426.6	357.3	<b>135.1</b>
MIS	6.571	6.522	2.174	<b>1.087</b>	2.174	509.5	366.5	256.8	224.1	<b>116.9</b>
MK	0.035	0.035	0.035	0.035	<b>0.000</b>	2.9	2.7	2.7	2.7	<b>1.5</b>
SC	0.595	0.314	<b>0.129</b>	0.129	0.611	61.7	55.0	<b>38.8</b>	38.8	45.7
TSP	7.344	3.804	1.894	0.592	<b>0.099</b>	843.3	668.0	488.7	346.3	<b>190.6</b>
VRP	2.777	1.710	1.710	1.710	<b>0.694</b>	265.1	154.6	154.4	154.4	<b>32.9</b>
	3.484	2.661	1.568	1.072	<b>0.544</b>	362.2	274.1	209.9	172.6	<b>80.0</b>

\* DEF1 corresponds to the solver’s default setting where the execution time limit is  $1 \times 1000$  seconds. Similarly, DEF2, DEF5 and DEF10 correspond to the solver’s default setting with  $2 \times 1000$ ,  $5 \times 1000$  and  $10 \times 1000$  seconds execution time respectively.

Table 2 is a collection of solution quality results by the proposed method with a 1000 seconds execution time limit. To demonstrate the significance of performance improvement, we allow the solver to run for 2-10 times the execution time (i.e., 2000-10000 seconds) in its default setting. It is revealed from the table that the proposed method (the GCN column) gains remarkable advantages to the solver’s default setting of the same time limit (the DEF1 column) on all testing problems. Compared to the default setting with 10000 seconds (the DEF10 column), the proposed framework still maintains an average better performance, indicating a 10 times acceleration in solution finding.

### 5.3 Generalization to larger instances

The graph embedding framework endows the model to train and test on MIP instances of different scales. This is important for MIP solving since there is hardly any good strategy to handle large-scale NP-hard MIP problems. To investigate this, we train our GCN model on small-scale MIP instances, and test its applicability in large-scale ones. Detailed statistics of small and large instances are reported in Appendix A. It is revealed from table 3 that the GCN model maintains an acceptable prediction accuracy degradation when problem scale differs in the training and testing phase. In addition, the prediction result is still useful to improve solver’s performance.

Table 3: Generalization ability of the solution prediction framework

		FCNF	CFL	GA	MIS	MK	SC	TSP	VRP	Average
Average Precision	GCN	0.653	0.837	0.963	0.091	0.789	0.878	0.396	0.358	0.621
	GCN-G*	0.675	0.801	0.873	0.104	0.786	0.843	0.343	0.321	0.593
Primal Gap (%)	DEF	4.585	1.942	4.633	3.409	0.035	0.498	6.895	2.626	3.078
	GCN	0.000	0.913	0.480	0.000	0.000	0.513	1.726	0.539	0.521
	GCN-G	2.119	0.000	0.000	0.000	0.000	0.390	4.300	0.910	0.965

\* GCN-G is the GCN model trained on small-scale MIP instances.

## 6 Conclusions

We presented a supervised solution prediction framework to explore the correlations between MIP formulation structure and its local optimality patterns. The key feature of the model is a tripartite graph representation for MIP, based on which graph embedding is used to extract connection information among variables, constraints and the objective function. Through extensive experimental evaluations on 8 types of distinct MIP problems, we demonstrate the effectiveness and generality of the GCN model in prediction accuracy. Incorporated in an initial cut to the MIP model, the prediction results help to accelerate SCIP’s solution finding process by 10 times on similar problems. This result is inspiring to practitioners who are facing routinely large-scale MIPs on which the solver’s execution time is unacceptably long and tedious.

## References

- [1] Tobias Achterberg. SCIP: solving constraint integer programs. *Mathematical Programming Computation*, 1(1):1–41, 2009.
- [2] Alejandro Marcos Alvarez, Quentin Louveaux, and Louis Wehenkel. A machine learning-based approximation of strong branching. *INFORMS Journal on Computing*, 29(1):185–195, 2017.
- [3] Yoshua Bengio, Andrea Lodi, and Antoine Prouvost. Machine learning for combinatorial optimization: a methodological tour d’horizon. *arXiv preprint arXiv:1811.06128*, 2018.
- [4] Tianqi Chen and Carlos Guestrin. Xgboost: A scalable tree boosting system. In *Proceedings of the 22nd ACM SIGKDD international conference on knowledge discovery and data mining*, pages 785–794. ACM, 2016.
- [5] Hanjun Dai, Elias Khalil, Yuyu Zhang, Bistra Dilkina, and Le Song. Learning combinatorial optimization algorithms over graphs. In *Advances in Neural Information Processing Systems*, pages 6348–6358, 2017.
- [6] Matteo Fischetti and Michele Monaci. Proximity search for 0-1 mixed-integer convex programming. *Journal of Heuristics*, 20(6):709–731, 2014.
- [7] He He, Hal Daume III, and Jason M Eisner. Learning to search in branch and bound algorithms. In *Advances in neural information processing systems*, pages 3293–3301, 2014.
- [8] Elias B Khalil, Bistra Dilkina, George L Nemhauser, Shabbir Ahmed, and Yufen Shao. Learning to run heuristics in tree search. In *26th International Joint Conference on Artificial Intelligence (IJCAI)*, 2017.

- [9] Elias Boutros Khalil, Pierre Le Bodic, Le Song, George L Nemhauser, and Bistra N Dilkina. Learning to branch in mixed integer programming. In *AAAI*, pages 724–731, 2016.
- [10] Wouter Kool, Herke van Hoof, and Max Welling. Attention, learn to solve routing problems! *arXiv preprint arXiv:1803.08475*, 2018.
- [11] WWM Kool and M Welling. Attention solves your tsp. *arXiv preprint arXiv:1803.08475*, 2018.
- [12] Markus Kruber, Marco E Lübecke, and Axel Parmentier. Learning when to use a decomposition. In *International Conference on AI and OR Techniques in Constraint Programming for Combinatorial Optimization Problems*, pages 202–210. Springer, 2017.
- [13] Zhuwen Li, Qifeng Chen, and Vladlen Koltun. Combinatorial optimization with graph convolutional networks and guided tree search. In *Advances in Neural Information Processing Systems*, pages 537–546, 2018.
- [14] Alejandro Marcos Alvarez, Louis Wehenkel, and Quentin Louveaux. Online learning for strong branching approximation in branch-and-bound. 2016.
- [15] MIPLIB 2017, 2018. <http://miplib.zib.de>.
- [16] Mohammadreza Nazari, Afshin Oroojlooy, Lawrence Snyder, and Martin Takc. Reinforcement learning for solving the vehicle routing problem. In *Advances in Neural Information Processing Systems*, pages 9839–9849, 2018.
- [17] F. Pedregosa, G. Varoquaux, A. Gramfort, V. Michel, B. Thirion, O. Grisel, M. Blondel, P. Prettenhofer, R. Weiss, V. Dubourg, J. Vanderplas, A. Passos, D. Cournapeau, M. Brucher, M. Perrot, and E. Duchesnay. Scikit-learn: Machine learning in Python. *Journal of Machine Learning Research*, 12:2825–2830, 2011.
- [18] Daniel Selsam, Matthew Lamm, Benedikt Bunz, Percy Liang, Leonardo de Moura, and David L Dill. Learning a sat solver from single-bit supervision. *arXiv preprint arXiv:1802.03685*, 2018.
- [19] Petar Velikovi, Guillem Cucurull, Arantxa Casanova, Adriana Romero, Pietro Lio, and Yoshua Bengio. Graph attention networks. *arXiv preprint arXiv:1710.10903*, 2017.
- [20] Oriol Vinyals, Meire Fortunato, and Navdeep Jaitly. Pointer networks. In *Advances in Neural Information Processing Systems*, pages 2692–2700, 2015.
- [21] Mu Zhu. Recall, precision and average precision. *Department of Statistics and Actuarial Science, University of Waterloo*, Waterloo, 2:30, 2004.

## Appendix A

In this appendix, we describe the variable node features, constraint node features, and edge features in detail. All the features are collected at the root node of the B&B search tree where presolving and root LP relaxation has completed.

Variable Features	Feature Description	count
Basic	variable type (is binary, general integer)	2
	objective function coefficients (original, positive, negative)	3
	number of non-zero coefficient in the constraint.	1
	number of up (down) locks.	2
LP	LP value ( $x_j, x_j - \lfloor x_j \rfloor, \lceil x_j \rceil - x_j$ )	3
	LP value is fractional	1
	pseudocosts (upwards, downwards, ratio, sum, product)	5
	global lower (upper) bound	2
	reduced cost	1
Structure	degree statistics (mean, stdev, min, max) of constraints that the variable has nonzero coefficients.	4
	maximum (minimum) ratio of positive (negative) LHS (RHS) value.	8
	positive (negative) coefficient statistics (count, mean, stdev, min, max) of variables in the constraints.	10
	coefficient statistics of variables in the constraints (sum, mean, stdev, max, min) with respect to three weighting schemes: unit weight, dual cost, inverse of the coefficients sum in the constraint.	15
Constraint Features		
Basic	constraint type (is singleton, aggregation, precedence, knapsack, logicor, general linear, AND, OR, XOR, linking, cardinality, variable bound)	12
	Left-hand-side (LHS) and right-hand-side (RHS)	2
	number of nonzero (positive, negative) entries in the constraint	3
LP	dual solution of the constraint	1
	basis status of the constraint in the LP solution	1
Structure	sum norm of absolute (positive, negative) values of coefficients	3
	variable coefficient statistics in the constraint (mean, stdev, min, max)	4
Edge Features		
Basic	original edge coefficient	1
	normalized edge coefficient	1

Table 4: Description of variable, constraint and edge features.

## Appendix B

In this appendix, we describe the MIP formulation for each of the 8 types of CO problems in the paper. Table 5 and 6 below summarize the number of variables, constraints, percentage of nonzeros in the coefficient matrix  $A$ , and the percentage of binary variables that takes value 1 in the optimal solution.

Table 5: Problem scale statistics for large-scale instances

	Num. of variables	Num. of constraints	Fraction of nonzeros in the coefficient matrix	Fraction of nonzeros in a feasible solution
FCNF	[2398, 3568]	[1402, 2078]	0.00118	0.02913
CFL	[28956, 28956]	[29336, 29336]	0.00014	0.01358
GA	[22400, 22400]	[600, 600]	0.00333	0.02500
MIS	[400, 400]	[19153, 19713]	0.00502	0.05815
MK	[765, 842]	[46, 51]	1.00000	0.02684
SC	[4500, 4500]	[3500, 3500]	0.03000	0.02602
TSP	[17689, 19600]	[17954, 19879]	0.00031	0.00737
VRP	[1764, 1764]	[1802, 1802]	0.00314	0.02963

Table 6: Problem scale statistics for small-scale instances

	Num. of variables	Num. of constraints	Fraction of nonzeros in the coefficient matrix	Fraction of nonzeros in a feasible solution
FCNF	[1702, 2640]	[996, 1533]	0.00163	0.03392
CFL	[1212, 1212]	[1312, 1312]	0.00303	0.08624
GA	[1152, 1152]	[108, 108]	0.01852	0.08333
MIS	[125, 125]	[1734, 1929]	0.01620	0.14572
MK	[315, 350]	[19, 21]	1.00000	0.07113
SC	[750, 750]	[550, 550]	0.05000	0.06533
TSP	[1296, 1600]	[1367, 1679]	0.00387	0.02697
VRP	[196, 196]	[206, 206]	0.02422	0.08069

### 6.1 Fixed Charge Network Flow:

Consider a directed graph  $\mathcal{G} = (\mathcal{V}, \mathcal{E})$ , where each node  $v \in \mathcal{V}$  has demand  $d_v$  and the demand is balanced in the graph:  $\sum_{v \in \mathcal{V}} d_v = 0$ . The capacity of an arc  $e \in \mathcal{E}$  is  $u_e > 0$  and the cost of an  $x_e > 0$  quantity flow on this arc has a cost  $f_e + c_e x_e$ .

**Decision variables:**

- $y_e$ : binary variable.  $y_e = 1$ , if arc  $e \in \mathcal{E}$  is used and  $y_e = 0$  otherwise.
- $x_e$ : continuous variable, flow quantity on arc  $e \in \mathcal{E}$ .

**Formulation:**

$$\min \sum_{e \in \mathcal{E}} (f_e y_e + c_e x_e) \quad (11)$$

$$\text{s.t. } \sum_{e \in \mathcal{E}(v, v)} - \sum_{e \in \mathcal{E}(v, \mathcal{V})} = d_v, \quad \forall v \in \mathcal{V}, \quad (12)$$

$$0 \leq x_e \leq u_e y_e, \quad \forall e \in \mathcal{E}, \quad (13)$$

$$y_e \in \{0, 1\}, \quad \forall e \in \mathcal{E}. \quad (14)$$

### 6.2 Capacitated Facility Location:

Suppose there are  $m$  facilities and  $n$  customers and we wish to satisfy the customers demand at minimum cost. Let  $f_i$  denote the fixed cost of building facility  $i \in \{1, \dots, m\}$  and  $c_{ij}$  the shipping

cost of products from facility  $i$  to customer  $j \in \{1, \dots, n\}$ . The demand of customer  $j$  is assumed to be  $d_j > 0$  and the capacity of facility  $i$  is assumed to be  $u_i > 0$ .

**Decision variables:**

- $x_j$ : binary variable.  $x_j = 1$  if facility  $j$  is built, and  $x_j = 0$  otherwise.
- $y_{ij}$ : continuous variable, the fraction of the demand  $d_j$  fulfilled by facility  $i$ .

**Formulation:**

$$\min \quad \sum_{i=1}^m \sum_{j=1}^n c_{ij} y_{ij} + \sum_{i=1}^m f_i x_i \quad (15)$$

$$\text{s.t.} \quad \sum_{i=1}^m y_{ij} = 1, \quad \forall j \in \{1, \dots, n\}, \quad (16)$$

$$\sum_{j=1}^n d_j y_{ij} \leq u_i x_i, \quad \forall i \in \{1, \dots, m\} \quad (17)$$

$$y_{ij} \geq 0, \quad \forall i \in \{1, \dots, m\}, j \in \{1, \dots, n\} \quad (18)$$

$$x_j \in \{0, 1\}, \quad \forall j \in \{1, \dots, n\}. \quad (19)$$

### 6.3 Generalized Assignment:

Suppose there are  $n$  tasks and  $m$  agents and we wish to assign the tasks to agents to maximize total revenue. Let  $p_{ij}$  denote the revenue of assigning task  $j$  to agent  $i$  and  $w_{ij}$  denote the resource consumed,  $i \in \{1, \dots, m\}, j \in \{1, \dots, n\}$ . The total resource of agent  $i$  is assumed to be  $t_i$ .

**Decision variables:**

- $x_{ij}$ : binary variable.  $x_{ij} = 1$  if task  $j$  is assigned to agent  $i$ , and  $x_{ij} = 0$  otherwise.

**Formulation:**

$$\max \quad \sum_{i=1}^m \sum_{j=1}^n p_{ij} x_{ij} \quad (20)$$

$$\text{s.t.} \quad \sum_{j=1}^n w_{ij} x_{ij} \leq t_i, \quad \forall i \in \{1, \dots, m\}, \quad (21)$$

$$\sum_{i=1}^m x_{ij} = 1, \quad \forall j \in \{1, \dots, n\}, \quad (22)$$

$$x_{ij} \in \{0, 1\}, \quad \forall i \in \{1, \dots, m\}, j \in \{1, \dots, n\}. \quad (23)$$

### 6.4 Maximal Independent Set:

Consider an undirected graph  $\mathcal{G} = (\mathcal{V}, \mathcal{E})$ , a subset of nodes  $\mathcal{S} \subseteq \mathcal{V}$  is called an independent set iff there is no edge between any pair of nodes in  $\mathcal{S}$ . The maximal independent set problem is to find an independent set in  $\mathcal{G}$  of maximum cardinality.

**Decision variables:**

- $x_v$ : binary variable.  $x_v = 1$  if node  $v \in \mathcal{V}$  is chosen in the independent set, and 0 otherwise.

**Formulation:**

$$\max \quad \sum_{v \in \mathcal{V}} x_v \quad (24)$$

$$\text{s.t.} \quad x_u + x_v \leq 1, \quad \forall (u, v) \in \mathcal{E}, \quad (25)$$

$$x_v \in \{0, 1\}, \quad \forall v \in \mathcal{V}. \quad (26)$$

## 6.5 Multidimensional Knapsack:

Consider a knapsack problem of  $n$  items with  $m$  dimensional capacity constraints. Let  $W_i$  denotes the capacity of the  $i$ -th dimension in the knapsack,  $p_j$  the profit of packing item  $j$ , and  $w_{ij}$  the size of item  $j$  in the  $i$ -th dimension,  $i \in \{1, \dots, m\}$ ,  $j \in \{1, \dots, n\}$ .

**Decision variables:**

- $x_j$ : binary variable.  $x_j = 1$  if item  $j$  is chosen in the knapsack, and 0 otherwise.

**Formulation:**

$$\max \quad \sum_{j=1}^n p_j x_j \quad (27)$$

$$\text{s.t.} \quad \sum_{j=1}^n w_{ij} x_j \leq W_i, \quad \forall i \in \{1, \dots, m\}, \quad (28)$$

$$x_j \in \{0, 1\}, \quad \forall j \in \{1, \dots, n\}. \quad (29)$$

## 6.6 Set Covering:

Given a finite set  $\mathcal{U}$  and a collection of  $n$  subsets  $\mathcal{S}_1, \dots, \mathcal{S}_n$  of  $\mathcal{U}$ , the set covering problem is to identify the fewest sets of which the union is  $\mathcal{U}$ .

**Decision variables:**

- $x_j$ : binary variable.  $x_j = 1$  if set  $j$  is chosen, and 0 otherwise.

**Formulation:**

$$\min \quad \sum_{j=1}^n x_j \quad (30)$$

$$\text{s.t.} \quad \sum_{j \in \{1, \dots, n\} | v \in \mathcal{S}_j} x_j \geq 1, \quad \forall v \in \mathcal{U}, \quad (31)$$

$$x_j \in \{0, 1\}, \quad \forall j \in \{1, \dots, n\}. \quad (32)$$

## 6.7 Traveling Salesman Problem

Given a list of  $n$  cities, the traveling salesman problem is to find a shortest route to visit each city and returns to the origin city. Let  $c_{ij}$  denotes the distance from city  $i$  to city  $j$  ( $i \neq j$ ,  $i, j \in \{1, \dots, n\}$ ). We use the well-known Miller-Tucker-Zemlin (MTZ) formulation to model the TSP.

**Decision variables:**

- $x_{ij}$ : binary variable.  $x_{ij} = 1$  city  $j$  is visited immediately after city  $i$ , and 0 otherwise.
- $u_j$ : continuous variable, indicating the that city  $j$  is the  $u_j$ -th visited city.

**Formulation:**

$$\min \quad \sum_{i=1}^n \sum_{j \neq i, j=1}^n c_{ij} x_{ij} \quad (33)$$

$$\text{s.t.} \quad \sum_{i=1, i \neq j}^n x_{ij} = 1, \quad \forall j \in \{1, \dots, n\}, \quad (34)$$

$$\sum_{j=1, j \neq i}^n x_{ij} = 1, \quad \forall i \in \{1, \dots, n\}, \quad (35)$$

$$u_i - u_j + nx_{ij} \leq n - 1, \quad \forall 2 \leq i \neq j \leq n, \quad (36)$$

$$0 \leq u_i \leq n - 1, \quad \forall i \in \{2, \dots, n\}, \quad (37)$$

$$x_{ij} \in \{0, 1\}, \quad \forall i, j \in \{1, \dots, n\}. \quad (38)$$

## 6.8 Vehicle Routing Problem

Given a set of  $n$  customers, the vehicle routing problem is to find the optimal set of routes to traverse in order to fulfill the demand of customers. To serve the customers, a fleet of  $K$  vehicles, each of which has a maximum capacity  $Q$  are provided. Let  $c_{ij}$  denotes the distance from customer  $i$  to customer  $j$  ( $i \neq j$ ,  $i, j \in \{0, \dots, n+1\}$ ).

### Decision variables:

- $x_{ij}$ : binary variable.  $x_{ij} = 1$  city  $j$  is visited immediately after city  $i$  by some vehicle, and 0 otherwise.
- $y_j$ : continuous variable, the cumulated demand on the route that visits node  $j$  up to this visit.

### Formulation:

$$\min \quad \sum_{i=0}^{n+1} \sum_{j=0}^{n+1} c_{ij} x_{ij} \quad (39)$$

$$\text{s.t.} \quad \sum_{j=1, j \neq i}^{n+1} x_{ij} = 1, \quad \forall i \in \{1, \dots, n\}, \quad (40)$$

$$\sum_{i=0, i \neq h}^n x_{ih} - \sum_{j=1, j \neq h}^{n+1} x_{hj} = 0, \quad \forall h \in \{1, \dots, n\}, \quad (41)$$

$$\sum_{j=1}^n x_{0j} \leq K, \quad (42)$$

$$y_j \geq y_i + q_j x_{ij} - Q(1 - x_{ij}), \quad \forall i, j \in \{0, \dots, n+1\} \quad (43)$$

$$0 \leq y_i \leq Q, \quad \forall i \in \{0, \dots, n+1\}, \quad (44)$$

$$x_{ij} \in \{0, 1\}, \quad \forall i, j \in \{0, \dots, n+1\}. \quad (45)$$